FOCUS PLASMA ELECTRON TEMPERATURE MEASUREMENT BY CONTINUUM INTENSITY ANALYSIS

by

MUHAMMAD ASIF

Department of Physics
Quaid-i-Azam University
Islamabad, Pakistan.

1995

This work is submitted as a dissertation
in partial fulfillment of
the requirements for the degree of

MASTER OF PHILOSOPHY
in
PHYSICS

Department of Physics
Quaid-i-Azam University
Islamabad, Pakistan.

This work is partially supported by the Pakistan Science Foundation
Project C-QU /Phys (92), Pakistan Atomic Energy Commission Project
for Plasma Physics and Quaid-i-Azam University Research Grant.

Certificate

Certified that the work contained in this dissertation was carried out by **Muhammad Asif** under my supervision.

Zaka-ullah

(Dr. M. Zakaullah)
Department of Physics
Quaid-i-Azam University
Islamabad, Pakistan.

Submitted through:

for Aslam Baig

(Prof. Dr. Kamaluddin Ahmed)
Chairman
Department of Physics
Quaid-i-Azam University
Islamabad, Pakistan.

DEDICATED TO

MY LOVING PARENTS, SISTERS AND BROTHER

Acknowledgments

In the name of Almighty Allah the most merciful and benevolent, the creator of the universe, who gave me the courage and strength to complete this dissertation. I offer my humblest thanks to his Prophet Mohammed (peace be upon him), who is forever a source of guidance and knowledge for humanity.

I feel great pleasure in expressing my profound thanks to my supervisor Dr. M. Zakaullah for his keen interest, constant encouragement, kind supervision and sympathetic attitude. A great debt of gratitude is extended to Prof. Dr. G. Murtaza for his kind guidance.

I am also grateful to Prof. Dr. Kamal-ud-Din Ahmed, Chairman Department of Physics for providing facilities to conduct the research work. I would also like to thank Dr. Sajjad Mahmood for his useful suggestions in improving the manuscript.

Special thanks are due to Dr. Arshad Majid Mirza, Dr. Suleman Qaisar, Mr.N.D.Khatak, Mr.M.Hanif Naseem Scientific Officer (PAEC), and Mr.Imtiaz Ahmad, who were always very helpful during my studies. I am also grateful to Mr.Khalid Alamger and Mr.Anwar Zeb Shah for their help during the experimental work.

I am extremely thankful and indebted to Mr.Shahzad Mahmood and Miss.Salma Khanum for their kind cooperation and useful suggestions during the preparation of the manuscript. Cordial thanks are also extended to

my colleagues Sharif, Abdul Majeed, Safdar, and Shafiq for their cooperation during that period.

Finally, I owe my profoundest gratitude to my parents, brother and sisters, and to all family members, who not only have always morally and financially supported but also inspired me to achieve high ideals of life.

Muhammad Asif

Abstract

The electron temperature of the focus plasma in a low energy Mather type device energized by 32μF, 15 kV (3.6) kJ single capacitor , with Hydrogen as the filling gas is estimated. The ratio of integrated bremsstrahlung emission transmitted through foils, to the total incident flux as a function of foil thickness at various temperature is obtained for foil absorbers of designated material, Aluminium in our case. Using 3, 6, 9 and 18 μm thick Aluminium absorbers, the transmitted X-ray flux is detected. By comparing the experimental and theoretical curves through a computer programme the plasma electron temperature is determined. Results show that the Hydrogen focus plasma electron temperature is about 580 eV.

Contents

Chapter 1

Introduction

In a plasma focus, high density ($\sim 10^{25} m^{-3}$) high temperature (~ 1 keV) plasma is formed. The process of measuring plasma density and temperature is normally very complicated, lengthy and time consuming. That is why, in most of the experiments on plasma focus, the attention is confined to neutron and X-ray emission. In this dissertation, the results of plasma electron temperature measurements by continuum radiations intensity analysis with Hydrogen as the filling gas, are presented.

1.1 Historical review

In order to heat the matter to Fusion temperature many efforts had been done in the early 1950's. High pulsed current was passed through ring-shaped and

straight discharge tubes filled with Hydrogen. It was speculated that the Hydrogen plasma will be heated by the virtue of current and isolated from the tube wall due to self generated magnetic field. When high current of the order of several hundred kilo ampere was passed through low density gaseous Deuterium which is an isotope of Hydrogen, intense neutron emission was observed. However further experiments did not confirm the conjectured thermonuclear origin of these neutrons. It was observed that the neutrons emission did not increase by increasing the current. The increase in discharge current just increased the impurity level in the plasma, introduced from the ceramic wall of the discharge chamber. It was inferred that addition of few tenths of 1% of high Z impurities in the Deuterium plasma suppress the hard radiation emission (neutrons and X-rays).

Filippov [1] was investigating the emission of hard radiations from high current discharges. He used a metal wall pinch tube equivalent in function to the linear Z-pinch device. This Metal chamber comprised of a Deuterium filled Copper tube 300 mm in diameter and 700 mm long into which two Copper electrodes 110 mm in diameter were inserted. Magnetic probe measurements of the dynamics of the plasma shell showed the occurrence of discharge in the vicinity of the insulator sleeve initially, which led to the constriction of plasma column near to the anode. From the measurements of the position of the neutron source with the help of a collimator, neutron source was found to reside close to the anode terminus. After repeated experiments, he inferred that if the cathode was eliminated, and the negative terminal of the capacitor bank was connected to the metal chamber

wall then the discharge remained unaffected. The resulting chamber was used for an extensive series of experiments on the compression zone of a non cylindrical pinch, which was named as **dense plasma focus** due to small axial spread and high concentration.

Mather [2] was working on a co-axial accelerator at Los Alamos Scientific Laboratory in U.S.A. He observed that under certain conditions high temperature dense plasma is formed in front of the anode. In this device too, the breakdown occurs initially across the insulator sleeve surface, and current sheath is developed, which is accelerated by magnetic pressure ($\vec{J} \times \vec{B}$) down the coaxial region. When this current reached at the end of anode, the radial collapse occurs due to the self generated azimuthal magnetic field. As a result a hot dense plasma is formed. The operation of the plasma focus which leads to the formation of dense and hot plasma can be subdivided into three phases. In the first phase, initial break down of the gas and formation of current sheath occurs. The second phase corresponds to axial run down of the uniform axially symmetric current sheath towards the open end of the accelerator (It does not occur in Filippov geometry). In the third phase, radial collapse of the azimuthally symmetric current sheath which collapses towards the axis to form very hot and dense plasma focus.

At Quaid-i-Azam university (QAU) Islamabad, a Mather type plasma focus device was designed and developed, which became operational during early 1988. This device is energized by a single 32μF, 15 kV (3.6 kJ) capacitor. Attention is paid to investigate the effects of different mechanical parameters like insulator

sleeve length [3] and Material [4], anode length [5], sequential focusing [6] and the effects of insulator sleeve contamination [7, 8].

1.2 Plasma electron temperature measurement

In the Laboratory, to obtain thermonuclear fusion, it is required to confine high density plasma at sufficiently high temperature for a sufficiently long time. Therefore the measurement of plasma temperature is one of the fundamental requirements in thermonuclear fusion research. Different techniques have been developed to measure the plasma electron temperature.

Jahoda et al., [9] measured the electron temperature by recording X-ray continuum transmission through metal foils of different thicknesses. They compared the experimental curve with the theoretical/numerical ones. This method to estimate the electron temperature requires lengthy computations, but has attracted much attention. This technique is followed in the present work. It will be described in detail, in chapter two.

Key [10] presented a method for electron temperature measurement based on X-ray Bremsstrahlung transmission as a function of absorber foil thickness. His theoretical estimates predict that the method is applicable in the energy range of 1 to 40 keV. It was further speculated that by deconvolution of the data, the X-ray spectrum as well as the electron energy distribution may be obtained. It

was because the transmitted X-ray intensity $S(t)$ is a function of the absorber thickness "t". The variation of the transmitted flux $S(\nu_c)$ with the absorber cutoff frequency ν_c gives the incident X-ray spectrum $I(\nu_c)$. The intensity of Bremsstralung or recombination continuous X-rays from a plasma after transmission through an absorber gives the X-ray absorption curve as a function of parameters other than its real thickness. Yoshinobu Matsukawa [11] also derived a simple analytic relation between the intensity of X-rays and the mass absorption coefficient of absorber material when the energy distribution of electrons is Maxwellian. This expression can be used to determine the electron temperature.

Donaldson [12] presented a theoretical analysis of foil absorption method to determine the plasma electron temperature. He suggested that by selecting appropriate foil parameters, measurement errors may be minimized. But the author ignored the contribution of line radiations due to high Z impurity ions in the plasma. There may be a situation where temperature is very low so that the detector's photon count rate fluctuations due to the low X-rays fluxes may become important. It introduces errors in determining the intensity ratio by two foil absorption technique, and may limit the accuracy of this method. In this case it would be better to measure the absolute X-ray intensity using a single foil absorber and to relate the transmitted flux to the plasma temperature through a suitable theoretical model.

The absolute temperature measurements require an exact knowledge of the solid angle subtended by the X-ray detector behind the foil absorber to the X-ray source

and an absolute calibration of the X-ray detector. Ahmad and Key [13] made use of this method along with the relative absorption method to measure temperature in Laser produced plasma. They concluded that the temperature values deduced from absolute measurement of soft X-ray flux transmitted through a metal foil are subjected to much less error than those deduced using the two foil absorption technique.

1.3 Layout of the dissertation

In this dissertation, a brief summary of Mather's and Filippov's original contribution to the development of plasma focus is described in chapter one. The review of plasma electron temperature measurements is presented in the same chapter. Different radiation mechanisms, that is free-free transitions, free-bound transitions and bound-bound transitions are presented in chapter two. A detailed description of plasma electron temperature measurement by continuum intensity analysis is also given in this chapter. The experimental setup and the diagnostics used in the experiment are described in chapter three. Chapter four contains the experimental results and concludes the dissertation.

Chapter 2

Plasma radiations

Different types of radiations are emitted from hot plasmas. These radiations include electromagnetic radiations, neutrons, electrons and ion beams as well as high energy neutral particles, that is atoms and molecules. The radiation emission from hot plasmas, though generating enormous energy loss, provide an excellent and non perturbing diagnostic tool. In studying the plasmas, it is almost impossible to forget about these radiations. The parameters which characterize a plasma, have a wide range of numerical values. Different experimental techniques employed to diagnose the plasmas depend on the plasma characteristics. These methods and techniques are usually complicated due to transient nature of the laboratory plasmas. The electromagnetic radiations which are emitted from plasmas include radiowaves; microwaves; infrared; visible; ultraviolet radiations and X-rays. The emission of these radiations is due to the interaction among ions,

electrons, atoms and molecules and due to interaction of these particles with electromagnetic fields.

Here we discuss briefly the electromagnetic radiation emission, which occurs mainly due to the following three mechanisms.

1. Bremsstrahlung radiations (free-free transitions)
2. Recombination radiations (free-bound transitions)
3. Line radiations (bound-bound transitions)

2.1 Bremsstrahlung radiations (free-free transitions)

According to classical electromagnetic theory, when a free electron moves in the field of an ion, it may be accelerated or retarded and it will radiate energy. These radiations are called Bremsstrahlung radiations. Since the electrons can have any energy before and after radiating the photon, the wavelength of these radiations vary continuously, and form a continuous spectrum, the shape of which depends upon the electron energy distribution i.e. the plasma temperature.

During the Bremsstrahlung process, an electron undergoes a "free-free transition" in the continuum of an ion. The radiation is emitted by the electron as a result of its acceleration in the Coulomb field of the ion. It may be considered as a

transition of an electron from a higher level to a lower level in the continuum of the ion. The energy lost during free-free transitions constitute a broad spectrum from X-rays to the optical region.

The photon energy hν released during a free-free transition is written according to the fundamental equation

$$h\nu = \frac{1}{2}mv^2 + \Delta E. \tag{2.1}$$

For Hydrogenic ions

$$\Delta E = \frac{Z^2 E_H}{p^2}, \tag{2.2}$$

where p is the effective quantum number of the level in the continuum, E_H is the ionization energy of the Hydrogen atom, ΔE is the energy difference corresponding to series limit E_∞ and the continuum level E_p, and $\frac{1}{2}mv^2$ is the kinetic energy of free electron before interaction with the ion. If the ionization energy of the species is larger than the photon energy, then the emission coefficient for free-free transition is given as [14]

$$\epsilon_{ff}(\omega) \approx \frac{16(\alpha a_0)^3}{3(3\pi)^{\frac{1}{2}}} E_H \left[\frac{E_H}{KT}\right]^{\frac{1}{2}} \exp\left[-\frac{\hbar\omega}{KT}\right] N_e \sum_{z,a} Z^2 N_a^Z, \tag{2.3}$$

where α is the structure constant, a_0 is the first Bohr radius, E_H is the binding energy of the Hydrogen atom, K is the Boltzman constant, $\hbar$ is the Planck's

constant divided by 2π, ω is the angular frequency, N_e is the density of electrons, Z is the charge number of the ions, and N_a^z is the total density of the ions of charge Z.

The power emitted per unit volume by Bremsstrahlung radiations is given as [14]

$$P_{ff}(\omega) \approx \frac{64}{3}\left[\frac{\pi}{3}\right]^{\frac{1}{2}}(\alpha a_0)^3 E_H \omega_H \left[\frac{KT}{E_H}\right]^{\frac{1}{2}} N_e \sum_{z,a} Z^2 N_a^z, \tag{2.4}$$

where $\omega_H = \frac{E_H}{\hbar} = 2 \cdot 06 \times 10^{16} \quad sec^{-1}$ is the angular frequency corresponding to the Lyman limit of Hydrogen. These two equations show that heavier elements are especially effective in producing Bremsstrahlung radiations at high temperature at which multiple ionization occurs.

To asses the importance of radiation cooling by Bremsstrahlung, it is convenient to consider the rate at which electrons loose their energy by this process. The corresponding rate coefficient is obtained by dividing the power emitted per unit volume. P_{ff} by $\frac{3}{2}N_e KT$ i.e.

$$R_{ff} \approx \frac{128}{9}\left[\frac{\pi}{3}\right]^{\frac{1}{2}}(\alpha a_0)^3 \omega_H \left[\frac{E_H}{KT}\right]^{\frac{1}{2}} \sum_{z,a} Z^2 N_a^z. \tag{2.5}$$

The terms used in the above equation have the same meanings as described in the last two equations. This rate coefficient is also proportional to the absolute density of impurity ions, that is the impurity ions cause more radiation losses.

For pure Hydrogen plasmas the Bremsstrahlung cooling rate coefficient can be

written as [14]

$$R_{ff} \approx \bar{g}_{ff} \frac{128}{9} \left[\frac{\pi}{3}\right]^{\frac{1}{2}} (\alpha a_0)^3 \omega_H \left[\frac{E_H}{KT}\right]^{\frac{1}{2}} N_e. \tag{2.6}$$

We have used averaged free-free Gaunt factor which represents the departure of the quantum mechanical calculation from the classical result. The plasma is considered quasineutral and the relation $\hbar\omega = KT$ is used. The above equation can be applied to all plasmas containing only singly ionized species. This equation gives the minimum radiation loss. Numerically the minimum cooling rate is

$$R_{min} \approx 1 \cdot 75 \times 10^{-20} \bar{g}_{ff} \left[\frac{E_H}{KT}\right]^{\frac{1}{2}} N_e \quad sec^{-1}. \tag{2.7}$$

Here the electron density N_e is measured in m^{-3} . For most experiments this loss rate would not cause any serious difficulty but the presence of heavy impurities enhance the radiation loss by a considerable factor.

2.2 Recombination radiations (free-bound transitions)

In the recombination process an electron of kinetic energy $\frac{1}{2}mv^2$ combines with an ion and forms a neutral atom in the excited or ground state. As a result, a

photon of energy hν is emitted. The opposite process is called photo ionization. This process can be written as

$$A^+ + e^- \rightleftharpoons h\nu + A^*, \tag{2.8}$$

where A^* is excited neutral atom and $h\nu$ is Photon energy which is related with binding energy ΔE and electron velocity v as

$$h\nu = \frac{1}{2}mv^2 + \Delta E. \tag{2.9}$$

It is clear from this equation that the photon energy depends upon the kinetic energy of the electron. As the electron can have any possible energy value so the photon may also have any energy value. The binding energy for Hydrogen like atoms is given by

$$\Delta E = \frac{Z^2 E_H}{p^2}, \tag{2.10}$$

where E_H is the ionization energy of Hydrogen atom, p is the effective quantum number of that level respectively and Z is the ionic charge. The rate at which this binary reaction process takes place per unit volume is proportional to the densities of both electrons and ions.

We may use the Hydrogenic ion approximation to calculate the radiative loss due to recombination radiations. The emission coefficient for free-bound transition is

[14]

$$\epsilon_{fb} \approx \frac{32(\alpha a_0)^3}{3(3\pi)^{\frac{1}{2}}} E_H \left[\frac{E_H}{KT}\right]^{\frac{3}{2}} exp\left[-\frac{\hbar\omega}{KT}\right] N_e \sum_{z,a,n} \frac{Z^4}{n^3} exp\left[\frac{Z^2 E_H}{Z^2 KT}\right] N_a^z. \qquad (2.11)$$

Here the terms used have the same meanings as describe in free-free transitions. In this expression Gaunt correction is ignored for simplicity. The power loss in free-bound transition is [14]

$$P_{fb} \approx \frac{128}{3}\left[\frac{\pi}{3}\right]^{\frac{1}{2}} (\alpha a_0)^3 \omega_H E_H \left[\frac{E_H}{KT}\right]^{\frac{1}{2}} N_e \sum_{z,a,n} \frac{Z^4}{n^3} N_a^z. \qquad (2.12)$$

If n_{min} is the minimum effective quantum number of the ground state of the atom or ion, then the term $\sum \frac{1}{n^3}$ is given by $\frac{1}{2n_{min}^2}$. Here n_{min} can be calculated as

$$n_{min} \approx \left[\frac{Z^2 E_H}{E_\infty^{z-1,a}}\right]^{\frac{1}{2}}, \qquad (2.13)$$

where $E_\infty^{z-1,a}$ is the ionization energy of ions with charge $z-1$ and 'a' is the atomic number. Therefore, the relation for the power radiated through free-bound transitions takes the form

$$p_{fb} \approx \frac{64}{3}\left[\frac{\pi}{3}\right]^{\frac{1}{2}} (\alpha a_0)^3 \omega_H E_H \left[\frac{KT}{E_H}\right]^{\frac{1}{2}} N_e \sum_{z,a} Z^2 \left[\frac{E_\infty^{z-1,a}}{KT}\right] N_a^z. \qquad (2.14)$$

If we compare the power radiated through free-bound transition with the power radiated through free-free transition then we see that free-bound contribution is

larger than free-free contribution for a given ion by a factor $\frac{E_{\infty}^{z-1,a}}{KT}$. At normal temperature, P_{fb} is 10 times larger than P_{ff}. The power loss by free-free transition can dominate the power loss by free-bound transition only if temperature is larger than $\frac{E_{\infty}^{z-1,a}}{K}$. It is important for light elements whose ions are completely stripped in high energy plasma. If the plasma contains the completely stripped ions only, which can not emit any line radiation and if we introduce appropriate average Gaunt factor , then power loss by free-free transitions and power loss by free-bound transitions given by the above two equations are true. So the total power loss per unit volume emitted by such a plasmas can be calculated as

$$\begin{aligned} P_{con} &= P_{ff} + P_{fb}, \\ P_{con} &\approx \frac{64}{3}\left[\frac{\pi}{3}\right]^{\frac{1}{2}}(\alpha a_0)^3 \omega_H E_H \left[\frac{KT}{E_H}\right]^{\frac{1}{2}} N_e \sum_{z,a} Z^2 \left[\bar{g}_{ff}^z + \frac{2Z^2 E_H}{KT}\bar{g}_{fb}^z\right] N_a^z . \quad (2.15) \end{aligned}$$

In this equation recombination into excited state is neglected, $\bar{g}_{ff}^z$ is the free-free Gaunt factor for Hydrogenic ions of charge Z and $\bar{g}_{fb}^z$ is the Gaunt factor of the Lyman continuum. The major contribution to the free-bound emission is from Lyman continuum. It is assumed that the Gaunt factors are slowly varying functions so the above procedure is sufficient for energy loss considerations.

The above equation is good for high energy plasmas, which always contain some impurity ions. At high temperature if all the ions are completely stripped, then relative cooling rate of the electron can be obtained by dividing the equation (2.15) by $\frac{3}{2}N_e KT$ and we get

$$R_{con} \approx \frac{128}{9}\left[\frac{\pi}{3}\right]^{\frac{1}{2}}(\alpha a_0)^3\omega_H\left[\frac{E_H}{KT}\right]^{\frac{1}{2}}\sum_{z,a} Z^2\left[\bar{g}^z_{ff} + \frac{2Z^2E_H}{KT}\bar{g}^z_{ff}\right]N^z_a. \qquad (2.16)$$

If the plasma is composed of Hydrogen and some impurity atoms, then this equation gives us minimum radiative cooling rate. Small admixture of impurity increases the minimum cooling rate due to strong Z dependence. For example one percent of Oxygen at 1.5 keV would increase the radiation losses by a factor of 3 and even more than 3 if temperature is low and line radiations are not completely eliminated. Practically for all laboratory plasmas self absorption of recombination radiation is negligible. It is not important for energy loss calculations. For numerical estimate the relative energy loss rate is calculated as

$$R_{con} \approx 1.75 * 10^{-20}\left[\frac{E_H}{KT}\right]^{\frac{1}{2}}\sum_{z,a} Z^2\left[\bar{g}^z_{ff} + \frac{2Z^2E_H}{KT}\bar{g}^z_{ff}\right]N^z_a \quad sec^{-1}, \qquad (2.17)$$

where ion densities are in m^{-3}

2.3 Line radiations (bound-bound transitions)

The line radiations are emitted from radiators (atoms, ions and molecules) due to inner transitions of the electrons. The radiators always try to remain in the stable state. So whenever these are in the exited state, dexcite to obtain the

stable state. In this process, electrons make the transitions between two bound levels. The extra energy possessed by the electron is released in the form of a photon. The energy of the photon which is released during dexcitation process is equal to the energy difference of the two levels i.e. the initial and final energy levels. The photons are emitted as discrete packets of energy and the spectrograph detects them as lines, that is why these radiations are called line radiations. These radiations are also known as characteristic radiations because the radiations provide information about the characteristics of the radiators (ions, atoms, or molecules).

The transitions between different energy levels give lines of different frequency. The spectra of line radiations may be grouped in certain series of lines. These lines are known as $K, L, M, ...series$. When transitions from higher orbits say $n = 2, 3, ...$ to K-shell occurs, we get K-series. Similarly if transition from higher orbit to L, M shell occurs we get L and M series respectively.

The intensity of each line is different from the other. The further classification of line radiations is termed as $\alpha - line$, $\beta - line$, $\gamma - line$, etc. The most intense line is named $\alpha - line$ and it is associated with $\Delta n = 1$ transitions. The line with decreasing intensities are termed as $\beta - line$ and $\gamma - line$ and are associated with $\Delta n = 2, 3$ transitions. The close analysis of $\alpha - line$ shows that it is not a single line but a combination of two lines of different intensities. The intensity of one line in the line pair is greater than the other line. Line radiative process are of two types [15].

1. Spontaneous emission

2. Stimulated emission

Spontaneous emission

An atom or molecule in an excited state always tries to obtain a stable configuration, when it is in the excited state i.e. in some upper energy level E_2 as given in the figure (2.1). It can not remain in the upper energy level for a long time and dexcites to a lower energy level E_1. During dexcitation the energy difference $E_2 - E_1$ is released in the form of an electromagnetic wave i.e. a photon. The emission of electromagnetic waves in this way are known as spontaneous emission. The energy of emitted photon is the product of Planck's constant 'h' and frequency of emitted photon ν i.e.

$$E_{upperlevel} - E_{lowerlevel} = h\nu. \tag{2.18}$$

The upper and lower energy levels could be any two out of the infinite set of energy levels possessed by an ion atom or a molecule. It has been noted that besides the electromagnetic decay, a radiation less transition may occur and gives up the energy difference in the form of kinetic energy of the surrounding atoms or molecules.

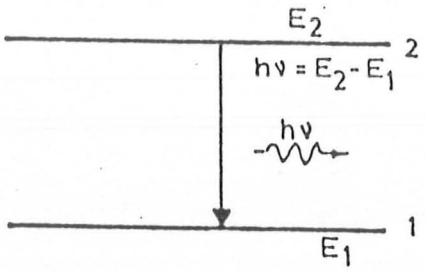

Figure 2.1: Two energy levels E_1, E_2; $E_2 > E_1$.

Stimulated emission

The phenomena of stimulated emission is some what different from spontaneous emission. If a photon of energy $h\nu$ is incident to an excited atom, it will stimulate the atom to undergo transition and emit a photon, provided the energy of the emitted photon is exactly equal to that of the incident photon. As a result we get two photons each of energy $h\nu$ and in phase with each other. This process is called stimulated emission and is shown in figure (2.2). So the major difference between the stimulated and spontaneous emission is that in stimulated emission there is a phase relation between incident photon and emitted photon and both moves in the same direction. But in case of spontaneous emission there is no phase relation between the photons emitted by various atoms of the material and these photons may have different directions of propagation.

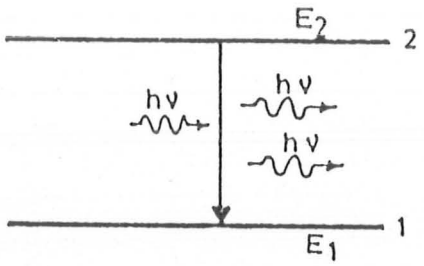

Figure 2.2: Stimulated emission of photons in phase with incident photon.

Power loss by line radiations

In a high temperature plasma the atoms of light elements such as Hydrogen or Helium are completely stripped and the line radiations are not possible by the transition of the electron between different energy levels. However, some high Z-impurity ions may be present in the plasma which are not completely stripped. These impurity ions give rise to line radiation. The power loss by line radiations due to impurity ion is given as [14]

$$P_{line}{}^{z-1,a} \approx 8\pi^{\frac{1}{2}}\alpha a_0^2 c E_H \left[\frac{E_H}{KT}\right]^{\frac{1}{2}} N_e N_1^{z-1,a} \sum_n f_{n1}^{z-1,a} exp\left[-\frac{E_n^{z-1,a}}{KT}\right], \qquad (2.19)$$

where $N_1^{z-1,a}$ is the ion density in the ground state, $f_{n1}^{z-1,a}$ is the oscillator strength and c is the velocity of light in free space.

A simplified expression for the power loss by the line radiations is given as [14]

$$P_{line}^{z-1,a} \approx 4\pi^{\frac{1}{2}} \alpha a_0^2 c E_H \left[\frac{E_H}{KT}\right]^{\frac{1}{2}} N_e N_a^{z-1,a} exp\left[-\frac{E_2^{z-1,a}}{KT}\right]. \qquad (2.20)$$

In this expression, summation over excited states is neglected and product of oscillator strength and ion density in the ground state is taken to be equal to the one half of the total density of the ions i.e.

$$f_{21}{}^{z-1,a} N_1^{z-1,a} \sim 0.5 N_a^{z-1}. \qquad (2.21)$$

The relative cooling rate of electrons through line radiations can be calculated if power loss by line radiations is divided by $\frac{3}{2} N_e KT$ and summed up over z.

Then we have

$$R_{line} \approx 8\frac{\pi^{\frac{1}{2}}}{3} \alpha a_0^2 c \left[\frac{E_H}{KT}\right]^{\frac{3}{2}} \sum_{z,a} N_a^{z-1} exp\left[-\frac{E_2^{z-1,a}}{KT}\right], \qquad (2.22)$$

which can be simplified to

$$R_{line} \approx 3 \times 10^{-8} \left[\frac{E_H}{KT}\right]^{\frac{3}{2}} \sum_{z,a} N_a^{z-1} exp\left[-\frac{E_2^{z-1,a}}{KT}\right] \quad sec^{-1}. \qquad (2.23)$$

Since completely stripped ions do not contribute to line radiations, so sum over z goes up only to $z = a$, where a is the charge number of the ions. In order to estimate the importance of the cooling rate of the line radiations we compare it with minimum Bremsstrahlung radiation emission rate, that is

$$\frac{R_{line}}{R_{min}} \approx \frac{1.7 \times 10^6}{\bar{g}_{ff}} \frac{E_H}{KT} \sum_{z,a} \frac{N_a^{z-1}}{N_e} exp\left[-\frac{E_2^{z-1,a}}{KT}\right]. \tag{2.24}$$

If we introduce as impurity one percent of Oxygen ions with only one electron at $KT = 1$ keV in the transient plasma, then the above ratio is nearly equal to 300. It means that impurity of Oxygen atoms increases the cooling rate through line radiations by 300 times. It is not in comparison with relative cooling rate due to continuum radiations by the impact of completely stripped Oxygen ions, which is increased only by a factor of 3 when the temperature is increased from 1 to 1.5 keV.

2.4 Electron temperature measurement

For thermonuclear Fusion in the laboratory, it is necessary to confine high density plasma at sufficiently high temperature for a sufficient long time. Thus the measurement of plasma temperature is one of the fundamental plasma diagnostic requirement. There are different methods and techniques for the determination of electron temperature. For example, by continuum intensity measurement and analysis, measurements of relative spectral line intensities, absorption of continuum radiations by a metal foil, and relative absorption of the continuum by a set of different metal foils etc. In the following, we will concentrate on the electron temperature measurement by a continuum intensity analysis.

A plasma emits electromagnetic radiation in a broad frequency range. These radiations include the line radiation as well as the continuous radiation. The later is associated with the acceleration of free electrons due to electrostatic interactions with the ions of the plasma, as well as to recombination processes. The former occurs at discrete frequencies, and are associated with the electronic transitions between bound energy levels of the atoms of the plasma. It is possible to determine the properties and characteristics of a plasma from the examination of these electromagnetic radiations emitted from the plasma. The intensity of the radiations at a given wavelength, or its spectral distribution over a given wavelength band can be determined experimentally and these measurement can be related to the relevant plasma parameters, that is electron concentration, electron and ion temperature etc. If the plasma temperature is greater than about 100 eV, most of the radiations from pure Deuterium plasma are Bremsstrahlung. The electron temperature can be estimated from the spectrum shape and the total radiated power. If impurities are present however, recombination and line radiations obscure the Bremsstrahlung radiation.

From a plasma of electron temperature T_e and electron number density N_e, ion number density N_a^Z of charge Z, the Bremsstrahlung radiation emission per unit frequency interval and per unit volume, is [9]

$$E_\nu = CN_eN_a^ZZ^2\left[\frac{E_H}{KT_e}\right]^{\frac{1}{2}}\bar{g}\exp\left[-\frac{h\nu}{KT_e}\right]. \tag{2.25}$$

Here

$$\begin{aligned} C &= 2^7\left[\frac{\pi}{3}\right]^{\frac{3}{2}}\alpha^3 E_H a_0^3, \\ &= 1.7\times 10^{-53} \quad J-m^3, \end{aligned} \tag{2.26}$$

where α is the fine structure constant, a_0 is the Bohr radius, E_H is the Hydrogen ionization potential, and $\bar{g}$ is the Gaunt factor, averaged over the Maxwell velocity distribution at electron temperature T_e. In term of wavelength this equation can be written as

$$E_\lambda = 1.9\times 10^{-22} N_e N_a^Z \bar{g}\left[KT_e\right]^{-\frac{1}{2}}\lambda^{-2}\exp\left[-\frac{12395}{\lambda KT_e}\right] \quad watts/m^3 - angstrom. \tag{2.27}$$

We can obtain the total radiated power from a Hydrogen plasma by integrating over all wavelengths

$$\int_0^\infty E_\lambda d\lambda = 1.5\times 10^{-26}\left[KT_e\right]^{\frac{1}{2}}\bar{g}N_e N_a^Z \quad watts - m^{-3}. \tag{2.28}$$

Here KT_e is in eV, and λ is in angstroms. The strong exponential dependence of the spectrum in the neighbourhood of the short wavelength cut off implies that the most sensitive temperature measurement can be made in the X-ray region. Measurement of the transmission of X-ray through absorbers of various thicknesses and materials is a technique for the spectral analysis of the incident

radiation. The transmitted X-ray flux through foils of absorption coefficients $\mu_i(E)$ may be written as [16]

$$I_\lambda \propto \lambda^{-2}\left[KT_e\right]^{-\frac{1}{2}} \exp\left[-\frac{E}{KT_e} - \sum_i \mu_i(E)t_i\right], \tag{2.29}$$

where the subscript i refers to the various foil materials, K is the Boltzmann constant, I_λ is the radiation flux intensity of wavelength λ, E is the photon energy and $\mu_i(E)$ is the mass absorption coefficient of the foil of thickness t_i.

We can write the ratio of the integrated bremsstrahlung emission transmitted through foils of the designated material to the total incident flux as

$$R = \frac{\sum dE_j \exp\left[-\frac{E_j}{KT} - \mu(E_j)t\right]}{\sum dE_j \exp\left[-\frac{E_j}{KT}\right]}, \tag{2.30}$$

where E_j refers to various photon energy. Using the data of Henke et al., [17] for Al, Ni and Cu foil absorbers (which are available in the laboratory), the above expression is determined by varying the foil thickness with the help of "Mathematica" on a 80486 computer, for different plasma temperatures, and results are presented in figure (2.3) to figure (2.5). We can also determine experimentally this expression for different foil thickness of designated materials. By comparing the theoretical and experimental curves through a computer programme the plasma electron temperature may be determined.

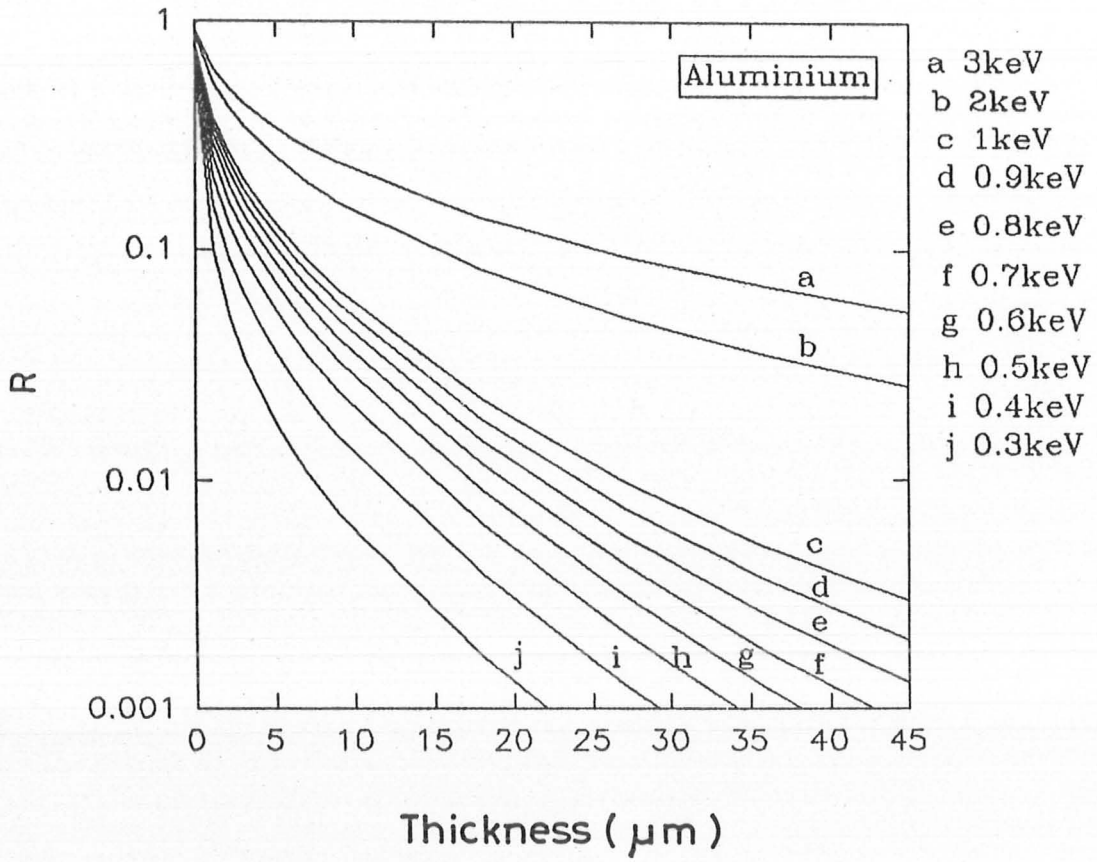

Figure 2.3: Ratio of the integrated bremsstrahlung emission transmitted through foil of Aluminum to the total incident flux versus foil thickness for various temperature.

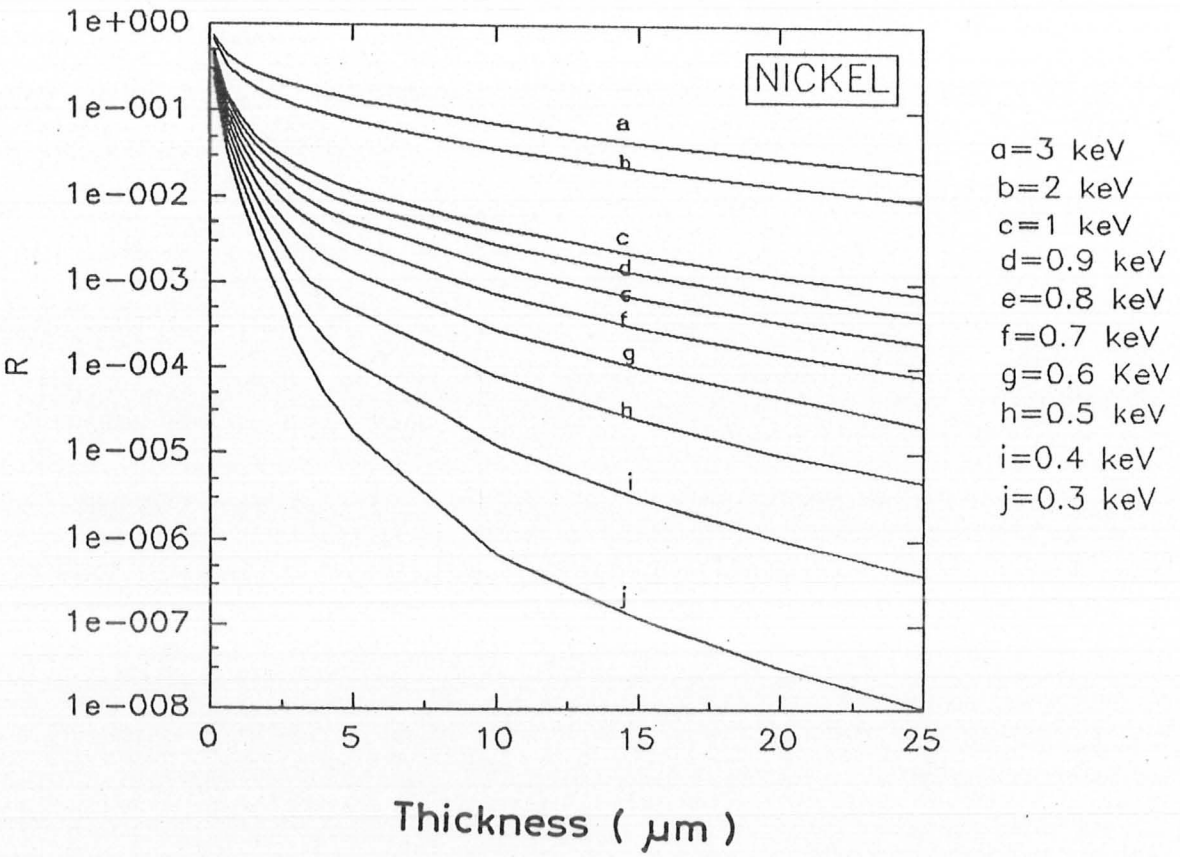

Figure 2.4: Ratio of the integrated bremsstrahlung emission transmitted through foil of Nickel to the total incident flux versus foil thickness for various temperature.

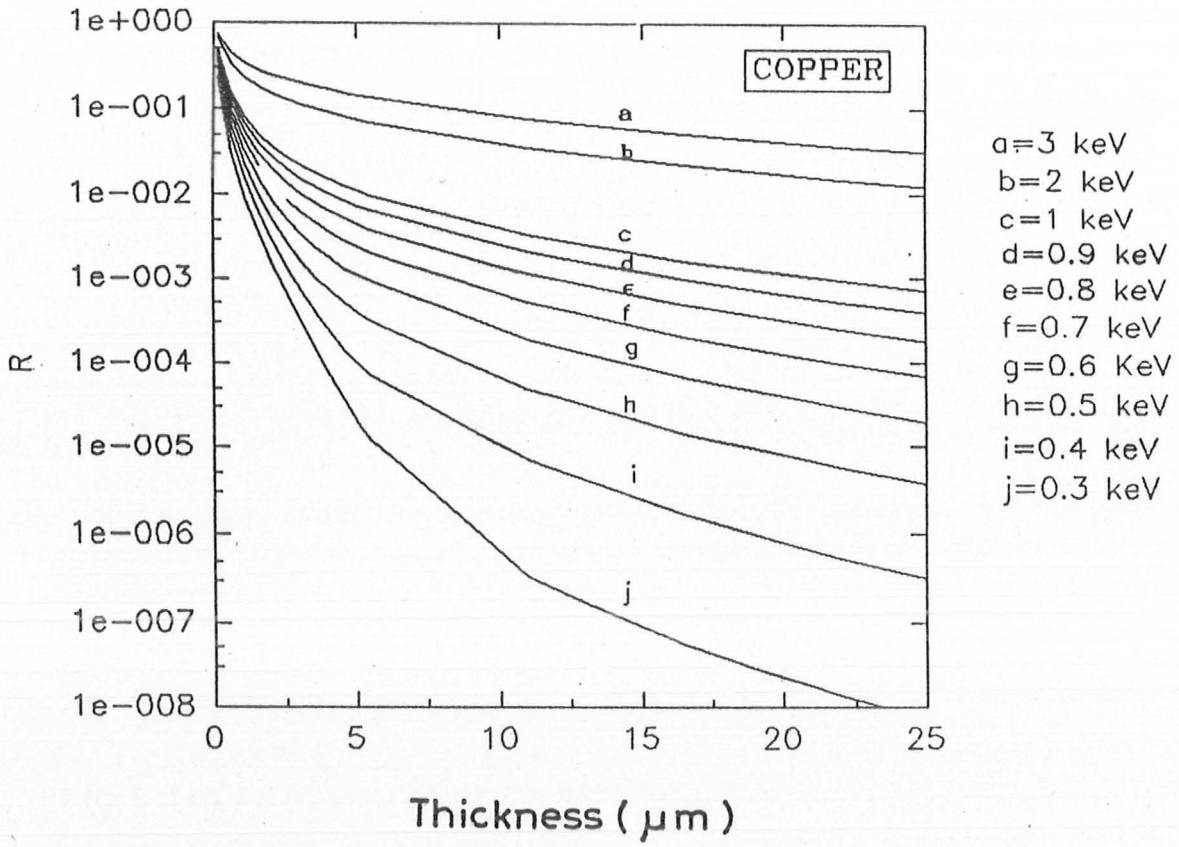

Figure 2.5: Ratio of the integrated bremsstrahlung emission transmitted through foil of Copper to the total incident flux versus foil thickness for various temperature.

Chapter 3

Experimental setup and diagnostics

In this chapter we discuss the experimental setup and the equipment, developed and used at Quaid-i-Azam University. This discussion includes a plasma focus system which mainly consists of the electrode system, energy storage and transfer system, trigger and dumping system. Some preliminary diagnostic tools like Rogowski coil, high voltage probe are also discussed. The pin-diodes which are used for X-ray detection, are described in the same chapter.

3.1 Plasma focus system

The plasma physics laboratory at Quaid-i-Azam University has a Mather type focus device operated by a single 32 μF, 15 kV capacitor. The maximum energy that can be discharged through the electrodes of plasma focus system is 3.6 kJ. But for safety, any electrical or electronic equipment should not be operated on its peak value. Due to these limitations, we charge the capacitor upto 12 kV and the total discharged energy through the plasma focus system per shot is 2.3 kJ.

3.1.1 Electrode system

It consists of a 160 mm long Cu rod of 18 mm diameter as anode which is surrounded by six 10 mm thick Cu rods forming the cathode with inner diameter of 50 mm. These cathode rods are screwed to a Cu plate with a knife edge near the anode. An insulator sleeve of Pyrex glass with breakdown length of 25 mm is placed between the anode and cathode as shown in the figure (3.1). A rubber disc of thickness 13 mm with a hole at its center is used to support the cylindrical glass sleeve so that it does not touch the anode or the cathode base plate. A Copper plate of diameter 285 mm and thickness 10 mm with a hole of 100 mm at its center, where a rubber disc is inserted, is called cathode header. There are eighteen steel screws which are used to connect the capacitor ground plate to the cathode header via coaxial cables. The central core of the coaxial cables connect the anode header and high voltage terminal. A Perspex disc of

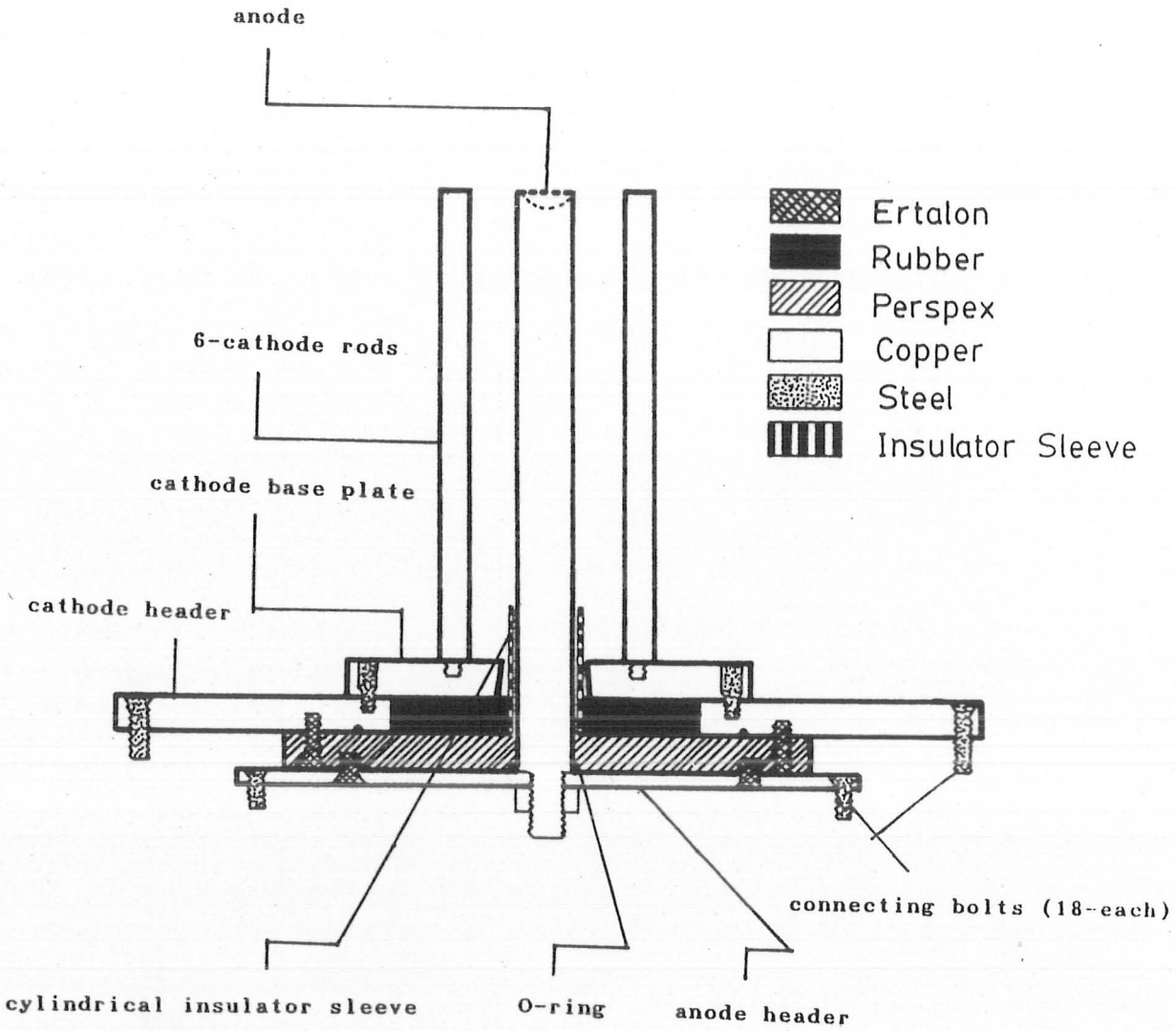

Figure 3.1: Plasma focus electrode assembly.

diameter smaller than anode header, along with sufficient layers of Myler and Polythene is inserted between the cathode and anode header to provide electrical insulation. The space around the Perspex plate is used to position a Rogowski coil to monitor the discharge current and system's inductance. In order to tighten the Perspex disc with anode and cathode header, special ertalon bolts are used. The schematic diagram of the electrode system is shown in figure (3.1).

3.1.2 Vacuum system and vacuum chamber

The electrode system is enclosed in a vacuum chamber, as shown in figure (3.2), which can be evacuated to the desired level. To produce the plasma, it is required to evacuate the vessel in which the plasma focus electrode system is seated. The vacuum system consists of a rotary vane pump along with an oil diffusion pump. Rotary pump can create a vacuum of the order of 10^{-2} mbar in half an hour. In addition to rotary pump, oil diffusion pump is also used, it can create vacuum of the order of 10^{-5} mbar in two hours. The vacuum chamber is a stainless steel container with six openings called ports. Each port is a channel through which plasma diagnostic is possible.

3.1.3 Energy storage and transfer system

Energy storage system which consists of a single capacitor of 32 μF, 15 kV is the vital part of the plasma focus system. The capacitor is energized with the help of

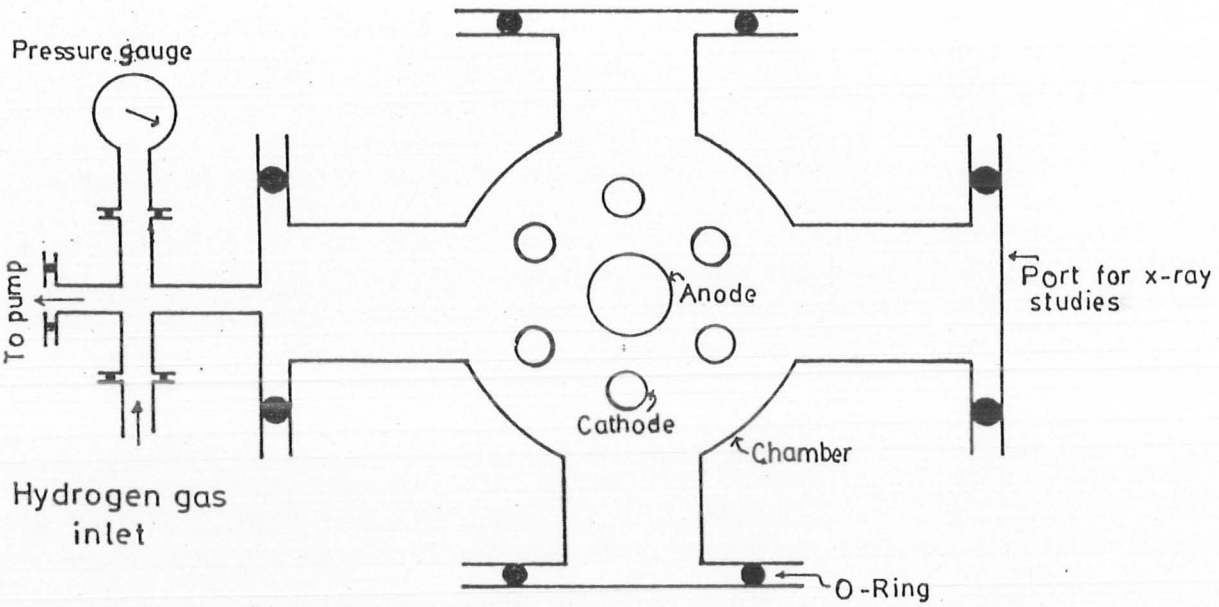

Figure 3.2: A schematic diagram showing plasma focus vacuum chamber.

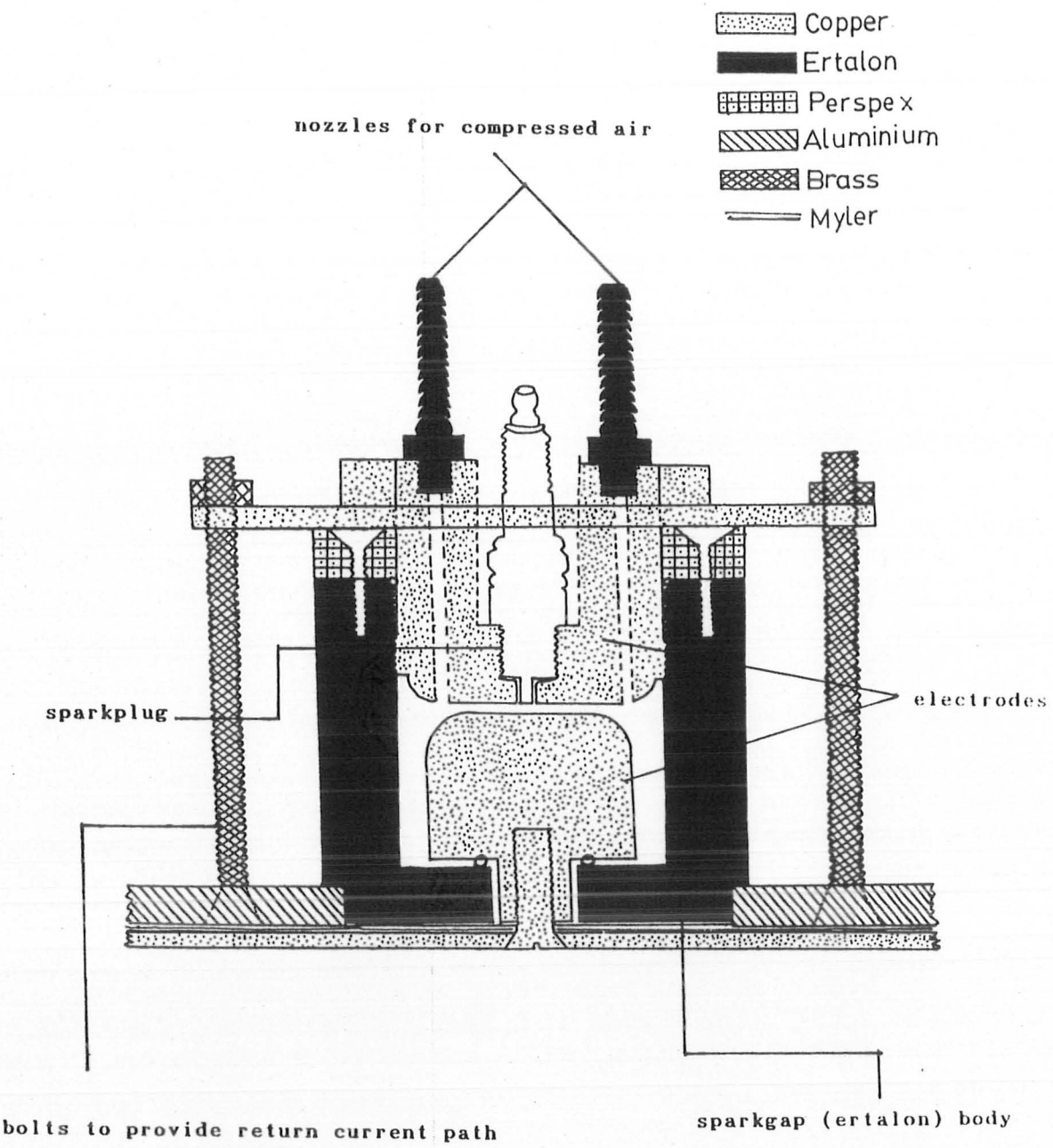

Figure 3.3: A schematic of pressurized sparkgap.

a charger ±25 kV, which can provide a current of 50 mA. The charger is provided with an automatic relay. When the capacitor is charged upto the required value, the charger is automatically switched off and ceases to function any more. Two Copper plates, 15 inches wide and $\frac{1}{8}$ inch thick are used to draw charge from the capacitor. These plates are placed one over the other to reduce the inductance. Sufficient layers of Myler and Polythene are inserted between the high voltage and ground plates for electrical insulation. A pressurized sparkgap [18] is employed as a switch which can handle a discharge current of about 200 kA, with a rise time less than one microsecond. The body of the sparkgap is machined from a Nylon rod of 100 mm diameter and the electrodes are developed from a 50 mm diameter Copper rod. A motor bike sparkplug with slight modification is used as a trigger pin. Six brass bolts tightened coaxially out side the sparkgap body provide a low inductance path to the circuit. The schematic of the sparkgap is given in figure (3.3). It is triggered by a −20 kV trigger pulse. A trigger pulse of −800 V is generated from SCR, which is further amplified upto −20 kV by a TV fly back transformer. A schematic of sparkgap trigger arrangement is shown in figure (3.4).

The sparkgap operation depends upon the pressure between the electrodes of the pressurized sparkgap. It works properly within 1.5 bar to 2.5 bar. At high pressure, the capacitor may not fire, while at low pressure, it may fire automatically. The energy stored in the capacitor is transferred to the focus device through eighteen coaxial cables of the shortest possible length (120 cm) connected in par-

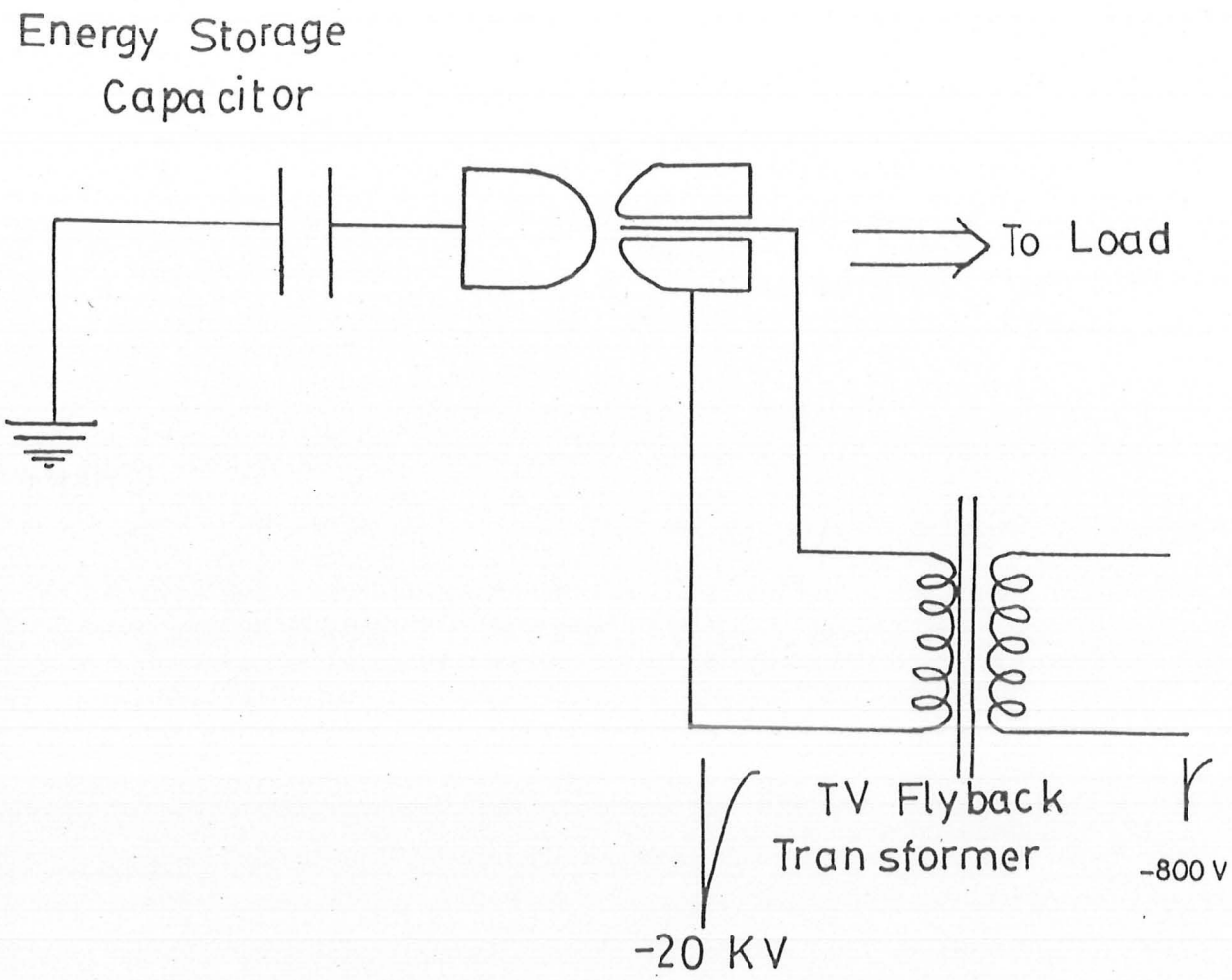

Figure 3.4: The sparkgap trigger arrangement.

allel. These cables connect the cathode and anode headers with the electrode of the sparkgap. With this configuration the measured parasitic inductance of the system is about 80 nH.

3.1.4 Dumping system

When we are working on the plasma focus, there is a possibility that due to some reasons, the discharge of the capacitor may not occur. It is dangerous to try to discharge the capacitor manually, as one needs to approach close to the capacitor. Therefore, an arrangement for discharging the capacitor is made by using a dumping system. It consists of an air pressure controlled plunger which in turn is connected to an air pressure controlled solenoid. This pneumatic plunger is used to connect high voltage and ground terminals, as shown in figure (3.5). The system is adjusted in such a way that when the solenoid is turned off the direction of air pressure becomes downward, and the earth is connected with the high voltage terminal through a 6 kΩ resistor. But when the solenoid is turned on, the direction of air pressure moves the plates P_1 and P_2 in upward direction, and the high voltage terminal and earth points are disconnected. There is also an arrangement through the internal circuit that when the system is dumped, the charger can not be switched on.

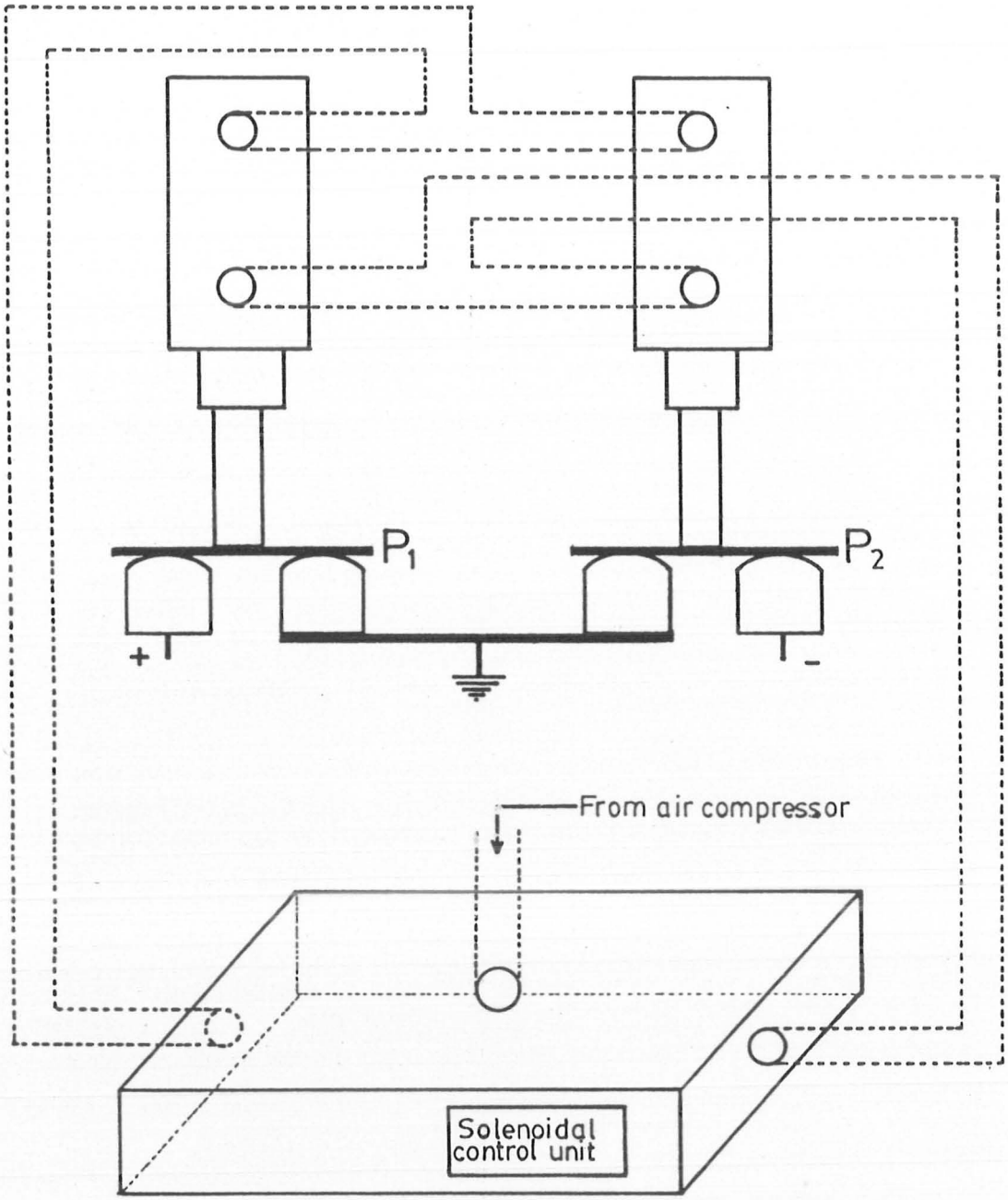

Figure 3.5: A schematic diagram of a dumping system.

3.1.5 Air pressure control

When the sparkgap is operated in open air, huge acoustic noise like a cracker blast is generated. To avoid this noise, the sparkgaps are sealed and filled with certain compressed gas or air. If the pressure between the two electrode is too low, the sparkgap may fire automatically, even before the capacitor is charged to the desired voltage. If the pressure is too high the sparkgap may not fire even when the trigger pulse is applied. So we need to tune the air pressure in the sparkgap. To this end we have employed a manometer. The compressed air tuned to the desired pressure enters the sparkgap through one nozzle and the other nozzle is connected to a manually controlled solenoidal valve. After every shot, the previous compressed air filled in the sparkgap is purged, so that the carbon impurities added during the sparkgap fire may be removed. If the previous compressed air is not purged the jitter in sparkgap firing is much increased and the sparkgap may also fire automatically, before the capacitor charging to the desired voltage is completed.

3.1.6 The trigger system

The trigger system is used to control the energy transfer from the main energy storage system to the electrodes of plasma focus device. A +3 V pulse is generated by discharging a small capacitor through handpressed switch. We apply this pulse to the gate of the silicon controlled rectifier (SCR). An SCR is a three junc-

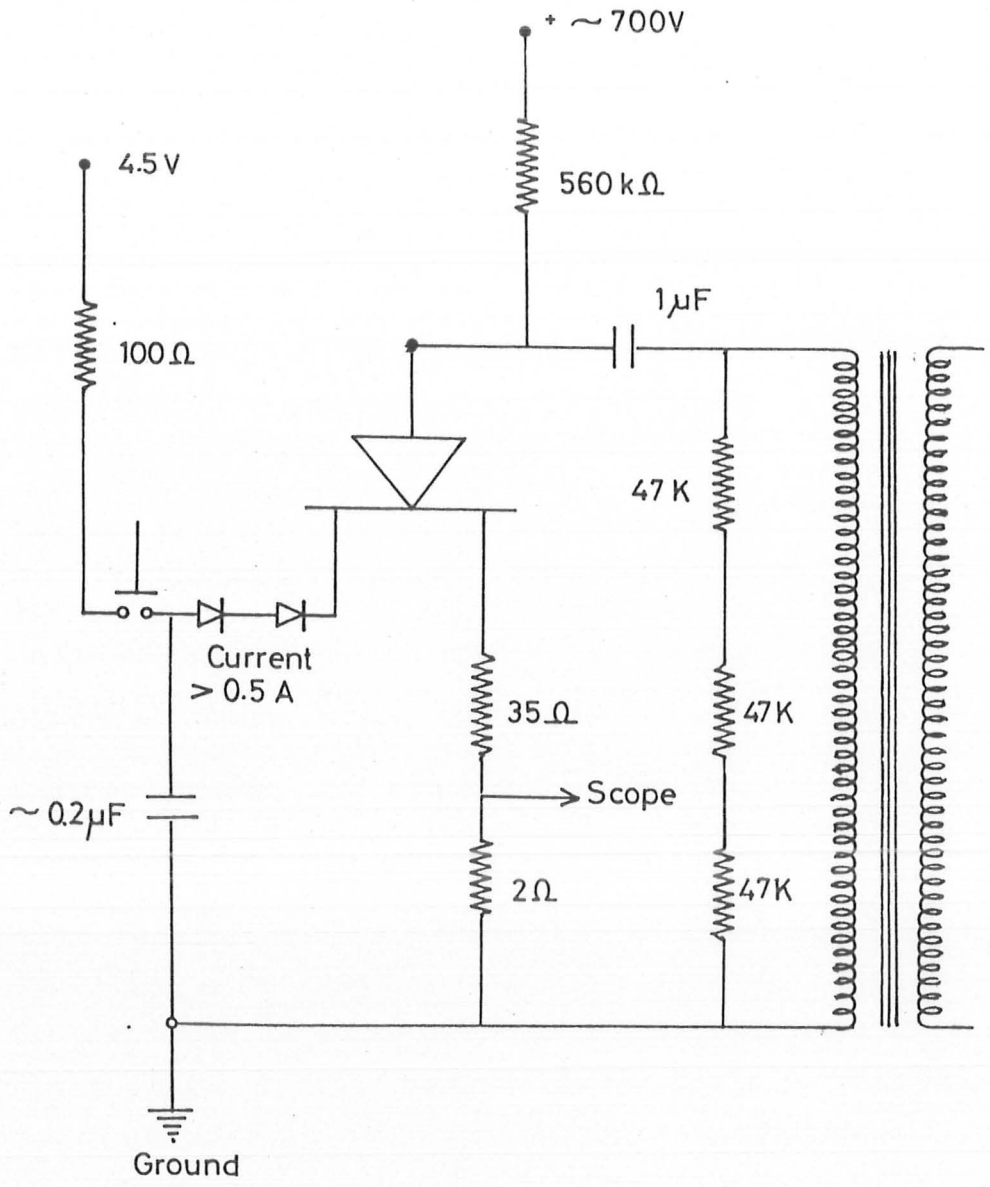

Figure 3.6: Circuit description of the SCR trigger unit.

tion semiconductor device with P-N-P-N configuration, its circuit arrangement is shown in figure (3.6). In this circuit arrangement the SCR generates a -800 V pulse and a $+30$ V pulse. The $+30$ V pulse is employed through an attenuator to trigger the oscilloscope. The -800 V pulse is amplified to -20 kV through a TV fly back transformer, which is than applied to sparkgap trigger pin. For the safety measure, the TV fly back transformer is dipped into caster oil, to enhance the electrical insulation.

3.2 Preliminary diagnostics

3.2.1 Rogowski coil

Rogowski coil is a device, which is used to measure high discharge current (few kA to few MA). We can not measure such a high current by other conventional electronic equipment. A Rogowski coil is a solenoidal coil whose ends are brought around together to form a torus. A schematic of Rogowski coil is shown in figure (3.7). Its working principle is based on the Faraday's law of electromagnetic induction. The length of solenoidal coil is kept very large as compared to the minor radius of the toroidal coil i.e. $l \gg r$. We assume that the magnetic field varies little one turn spacing, that is,

$$\frac{|\nabla B|}{|B|} \ll n, \tag{3.1}$$

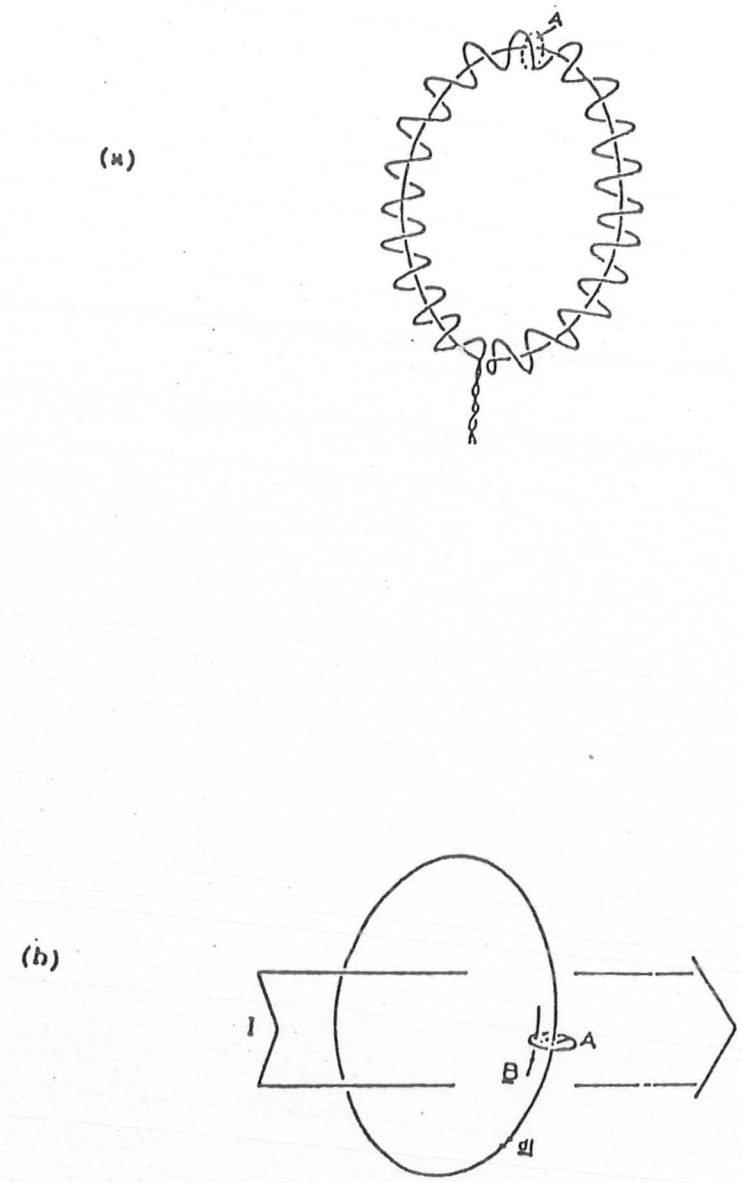

Figure 3.7: A schematic of Rogowski coil.

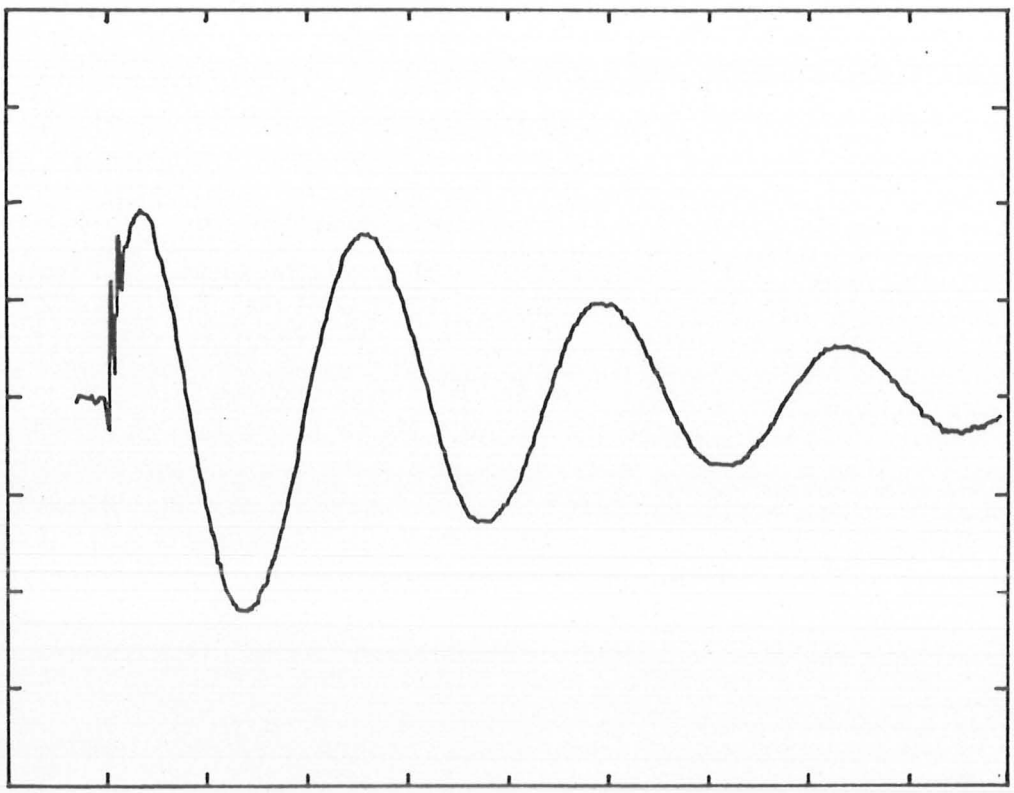

Figure 3.8: A typical Rogowski coil signal; 0.5 v/div, 5 μsec/div.

where n is the number of turns per unit length of the solenoid. If the current flow is far inside the coil, then the magnetic induction B associated with the Rogowski coil can be calculated from the Ampere's law.

$$\oint \vec{B}.\vec{dl} = \mu_o I. \tag{3.2}$$

Here μ_o is the magnetic permeability of free space and I is the current passing through the torus. Since I is a function of time in Mather's type plasma focus system, therefore induced magnetic field B would also be time dependent. From equation (3.2), we get

$$B(t) = \frac{\mu_o I(t)}{2\pi r}, \tag{3.3}$$

where r is the major radius of the toroidal coil. The magnetic flux ϕ linked to all turns of the coil is

$$\Phi = NBA, \tag{3.4}$$

Here N is the total number of turns of the coil, and A is the cross sectional area of each turn. The induced voltage at the terminals of the coil is given as

$$V_o(t) = -\frac{d\Phi}{dt}. \tag{3.5}$$

Using equations (3.3), (3.4) in the above equation, we get

$$V_o(t) = -\frac{\mu_o N A}{2\pi r}\frac{dI}{dt}. \tag{3.6}$$

Since induced voltage is proportional to the time rate of change of current. This induced voltage is integrated electronically to get a signal proportional to I .We use an RC integrator circuit to integrate the signal developed across the coil. The expression for the out put voltage is then given by

$$V(t) = \frac{1}{RC}\int_0^t V_o(t)dt, \tag{3.7}$$

where RC is the time constant of the integrator circuit. Using (3.6), we obtain the output voltage recorded by the oscilloscope.

$$V(t) = \frac{\mu_o N A I(t)}{2\pi r RC}, \tag{3.8}$$

We can measure total discharge current by measuring this voltage. But the voltage that appears on the oscilloscope is some what less than the actual value due to the attenuation of the connecting cables and other components used. So we need to calibrate the Rogowski coil for the precision of current measurements. When the plasma focus device is operated by shortening the cathode and anode, at the closed end, it has a very close analogy to the discharge of a capacitor

through fixed inductance L_0 and resistance R_0 . In such a circuit, the current is given by

$$I(t) = I_o \sin\left[\sqrt{\left(\frac{1}{L_oC_o} - \frac{R_o^2}{4L_o^2}\right)}t\right] \exp\left(-\frac{R_o t}{2L_o}\right). \tag{3.9}$$

Here L_0, C_0 and R_0 are the inductance, capacitance and resistance of the circuit respectively. In the plasma discharge

$$\frac{1}{L_oC_o} \gg \frac{R_o^2}{4L_o^2}. \tag{3.10}$$

So equation (3.9) can be simplified as

$$I(t) = I_o \sin\left[\frac{t}{\sqrt{L_oC_o}}\right] \exp\left(-\frac{R_o t}{2L_o}\right). \tag{3.11}$$

This equation shows that the signal is like a damped sinusoid, which means that the current signal oscillates sinusoidally, and its amplitude goes on decreasing with time. If T is the time period of RLC oscillatory circuit, then the voltage changes from V_0 to $-V_1$ during the first half cycle, provided that the first positive peak is taken as reference point and V_1 is always less than V_0. The amount of charge that flows through the circuit during the first half cycle is given by

$$Q = C_oV_o + C_oV_1$$

$$
\begin{aligned}
&= C_o V_o \left[1 + \frac{V_1}{V_o}\right] \\
&= C_o V_o [1 + f], \qquad (3.12)
\end{aligned}
$$

where $f = \frac{V_1}{V_0}$ is called the reversal ratio and is always less than unity. The value of peak current flowing through the circuit can be calculated from the equation

$$
\begin{aligned}
I_o(t) &= \frac{\omega}{2} C_o V_o [1 + f] \\
&= \pi \nu C_o V_o [1 + f] \\
&= \frac{\pi C_o V_o (1 + f)}{T}. \qquad (3.13)
\end{aligned}
$$

If we know the charging voltage of the capacitor, the peak current can be measured. The external inductance of the circuit can also be calculated by using the formula.

$$
\begin{aligned}
\omega &= \frac{1}{\sqrt{L_o C_o}}, \\
2\pi f &= \frac{1}{\sqrt{L_o C_o}}, \\
T &= 2\pi \sqrt{L_o C_o}, \qquad (3.14)
\end{aligned}
$$

where C_0 is the capacitance of the bank, L_0 is the parasitic inductance and T is the oscillation period observed by the oscilloscope. A typical Rogowski coil signal from plasma focus is as shown in figure (3.8).

3.2.2 High voltage probe

High voltage probe is a device, which is used to measure a high voltage which is developed due to rapid change in inductance during the radial collapse of the current sheath beyond the face of the central electrode in the plasma focus device. Because this voltage is several times the charging voltage, such a high voltage can not measured by conventional equipment. The high voltage probe is a resistor divider made by a chain of eleven resistors, normally 10 pieces of 510 Ω and one piece of 50 Ω across which the voltage is recorded . The power rating of each resistor is $1watt$. These resistors are connected in series for the safety of oscilloscope. In case of one resistor, if it is damaged, it may be shorted or opened. If it is short circuited, the high voltage will be appear on the oscilloscope causing a serious damage. When we use more than one resistors in series, then if one or two resistors are damaged and short circuited, the others protect the oscilloscope. The probability that all the ten resistors are damaged and short circuited is very small. The schematic of a high voltage probe is given in figure (3.9). The high voltage probe can not be connected directly to the plasma focus. It is connected across the cathode and anode headers. While connecting high voltage probe with the system, attention should be paid to insulate the high voltage point and the Copper casing which is at the ground potential. A typical high voltage signal is shown in figure (3.10).

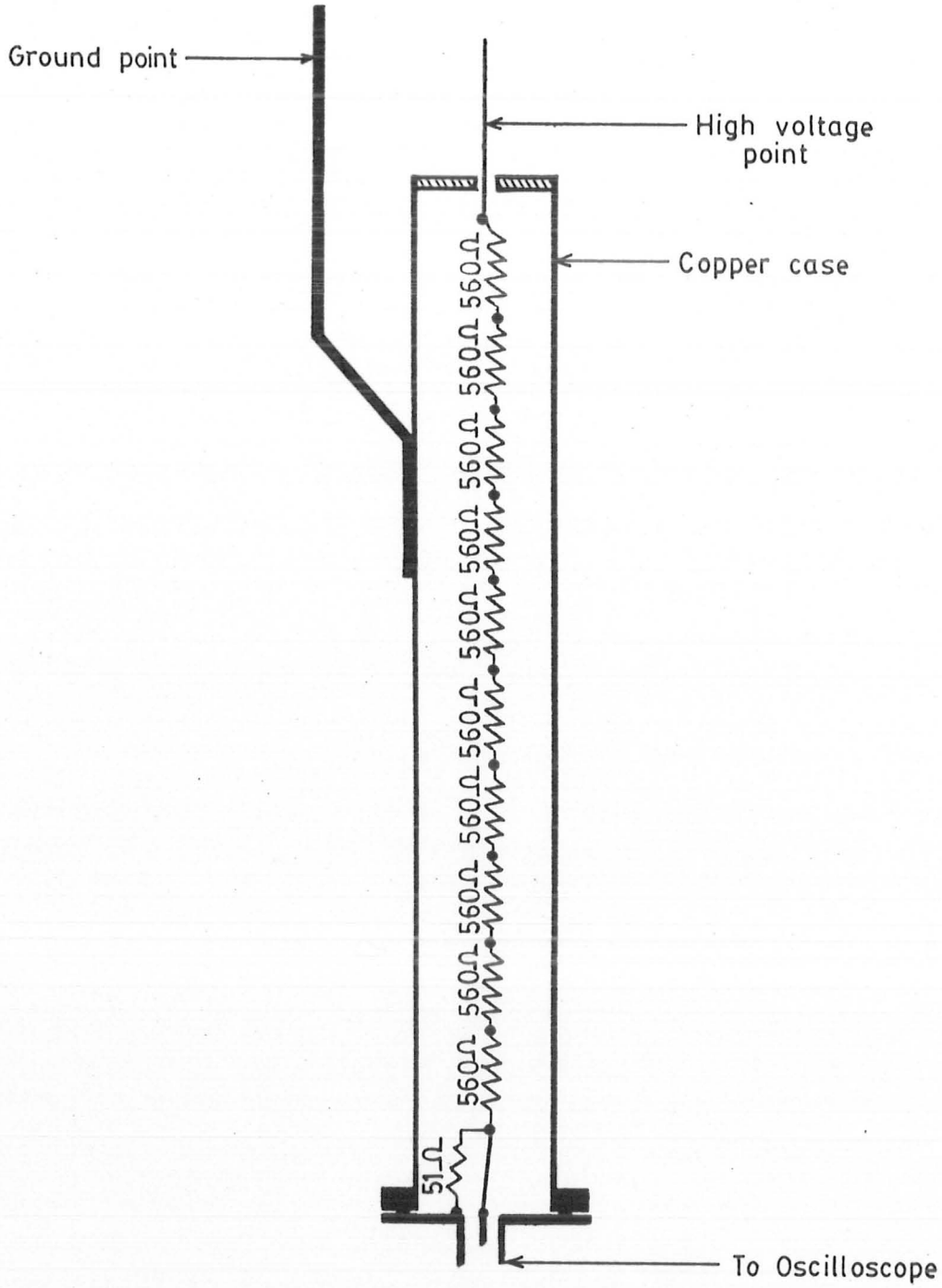

Figure 3.9: A schematic of high voltage probe.

Figure 3.10: A typical HV probe signal; 1 v/div, 0.5 μsec/div.

3.2.3 The PIN diodes assembly

A multi channel PIN diodes assembly is employed to record the X-ray pulses from the focus plasma. The BPX 65 PIN diodes are used in the experiment.

The typical characteristics of the diodes are:

Effective detection area	$1mm^2$,
Intrinsic Si layer thickness	$10\mu m$,
Rise time	$0.5nsec$,
Power dissipation	250 $mWatt$,
Breakdown voltage	$50V$.

Each diode is contained inside a metal casing with a glass window. This glass window is removed whereas suitable light-tight metals foils cover the diodes for the purpose of X-ray detection. These foils inhibit the optical radiation to approach the active area and attenuate the X-rays also. The diode has two connected leads, one positive and the other negative. The negative lead is common to the metal casing containing the diode. Each diode is reverse biased at 45 volts with a circuit shown in figure (3.11).

Three PIN diodes are adjusted into three good fit holes on a circular Aluminium plate (diameter 7cm, thickness 1.5 cm) with one of the diodes situated at the center of the plate as shown in figure (3.12). This Aluminium plate is attached with a stainless steel plate with the help of two brass rods with their ends threaded. The

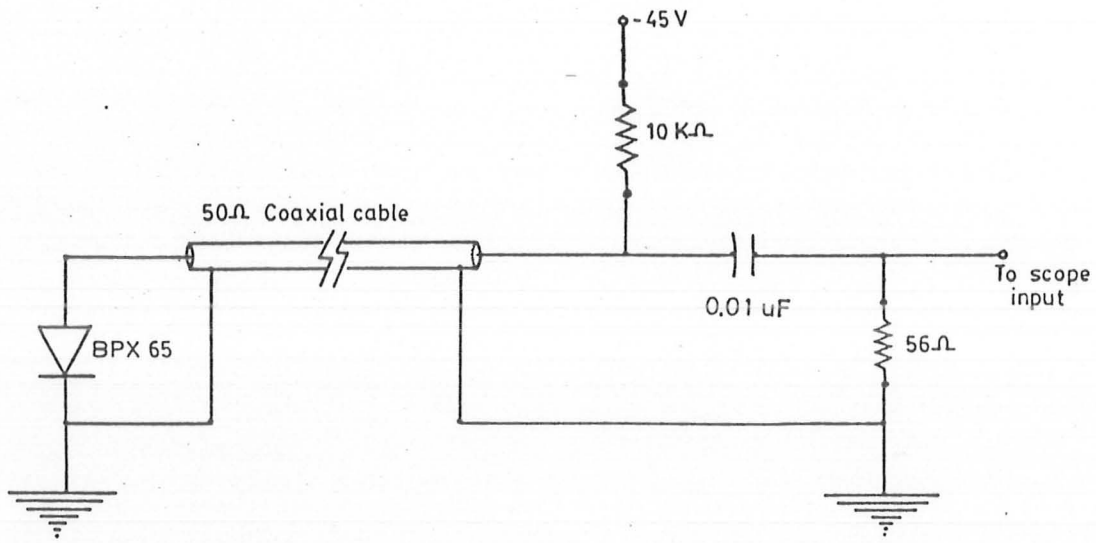

Figure 3.11: Biasing circuit of a PIN diode, for X-ray detection.

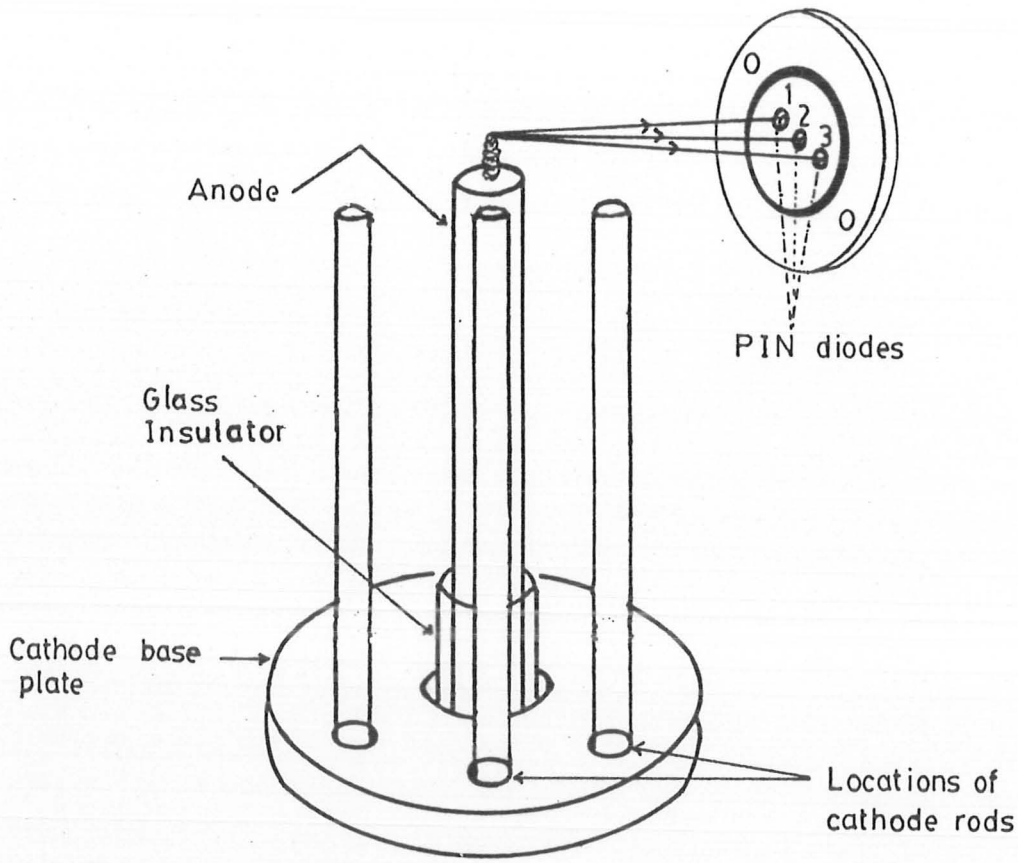

Figure 3.12: A schematic arrangement of PIN diodes assembly.

stainless steel plate has three good fit holes for three BNC sockets. These holes are made vacuum tight with O-rings to give a good vacuum which is required for the experiment.

The terminals of the diodes are connected to these BNC sockets via coaxial cables. These diodes may be called as channel 1, 2, 3. These channels are covered with Al, Ni, and Cu foils of appropriate thickness.

The PIN diodes assembly is mounted on the port in such a way that orientation of each diode is along a straight line perpendicular to the axis of the focus and all of the three diodes approximately view the same point. The distance between the center of the diode and tip of the central anode is kept about 1 cm.

Chapter 4

Results and conclusions

The focus plasma electron temperature in a low energy Mather type device energized by 32 μF, 15 kV (3.6 kJ) single capacitor, with Hydrogen as the filling gas is estimated by analysis of continuum X-rays emitted from the focus region.

4.1 Experimental results

During the experiment a multi-channel pin diodes assembly is employed to record X-rays from the focus plasma. The BPX 65 PIN diodes with some modification are used as detectors in the experiment. The safety glass covers of the diodes were removed, to enable the X-rays to reach the active area. To stop the optical radiations metal foils of appropriate thickness were employed. According to availability of the foils, the following sets are selected:

Al: $3\mu m, 6\mu m, 9\mu m, 18\mu m,$

Cu : $5.5\mu m, 11\mu m, 16.5\mu m, 22\mu m,$

Ni : $5\mu m, 10\mu m, 15\mu m, 20\mu m,$

The Hydrogen gas was used for plasma generation. The signals of the detectors covered with Cu foils of thickness $\geq 11\mu$m, and Ni foils of thickness $\geq 10\mu$m were weak, and signal to noise ratio was approaching unity. Therefore, the plasma electron temperature estimate was possible with only signals of the diode covered with Aluminium filter. A typical set of diode signals, when these were covered with 9 μm Al, 5 μm Ni and 5.5 μm Cu is presented in figure (4.1). These signals were recorded by 200 MHz, 4 channel GOULD digital storage oscilloscope. For every selected Aluminium foil, twenty shots were recorded. The average of X-ray signals intensity (ratio of X-ray flux transmitted through the foil to the incident flux) for each foil thickness are plotted against the foil thickness. The experimental curve is compared with the theoretical set of curves described in figure. The comparison is depicted in figure (4.2) and figure (4.3). For curve fitting, the χ^2 test is employed with the help of a 40486 personal computer,

where

$$\chi^2 = \sum_{j=1}^{n} \frac{\left[R_{exp}(x_j) - R_{th}(x_j)\right]^2}{R_{th}(x_j)} \tag{4.1}$$

The values of χ^2 at various temperatures are given in table (4.1). The best fit (minimum χ^2) is established for 580 eV.

4.2 Discussion and conclusion

The measurement of plasma temperature is one of the fundamental requirements in thermonuclear fusion research. The temperature of the focus plasma with Hydrogen as the filling gas, when the Mather type plasma focus is energized by a 32 μF, 15 kV (3.6) kJ single capacitor is measured by the technique of X-ray continuum intensity attenuation with different metal foil absorbers. The best fit of experimental and theoretical curves is found at 580 eV.

Mather [19] reported the focus plasma electron temperature measurement using pure Deutrium as the filling gas. His estimates for temperature lies within the range of $1-3$ keV. No results are available about Hydrogen focus plasma temperature for comparison with the present experiment. In plasma physics laboratory, Quaid-i-Azam University, the results of Deutrium plasma electron temperature measurement are not complete yet. However, the X-ray signal intensity from Deutrium focus plasma is an order of magnitude higher than from Hydrogen focus plasma. This interesting result needs further investigation.

To conclude, the focus plasma electron temperature with Hydrogen as a filling gas in a low energy Mather type plasma focus energized by 32 μF, 15 kV single capacitor is estimated. To this end, the method of attenuation of continuum X-ray flux through different thickness metal foil is followed. The experimental and theoretical curves are compared with the help of 80486 personal computer. The focus plasma electron temperature is found to be 580 eV.

Table 4.1: **The values of χ^2 at various temperatures.**

Temperature	χ^2
0.3 keV	4.4563×10^{-1}
0.4 keV	9.347×10^{-2}
0.5 keV	1.367×10^{-2}
0.55 keV	2.94×10^{-3}
0.56 keV	2.04×10^{-3}
0.57 keV	1.43×10^{-3}
0.58 keV	1.07×10^{-3}
0.59 keV	1.08×10^{-3}
0.6 keV	1.20×10^{-3}
0.61 keV	1.61×10^{-3}
0.7 keV	1.204×10^{-2}
0.8 keV	3.304×10^{-2}
0.9 kev	5.958×10^{-2}
1 kev	9.004×10^{-2}
2 keV	4.4893×10^{-1}
3 keV	7.4214×10^{-1}

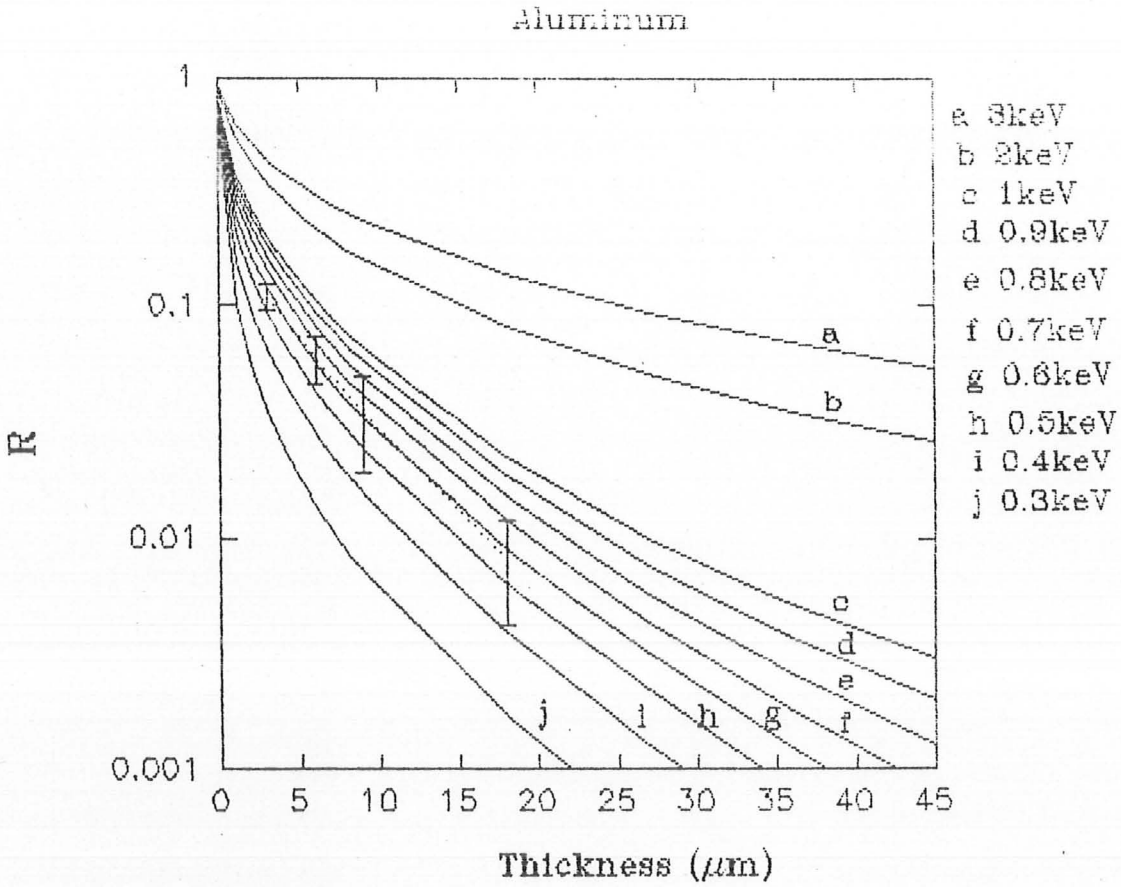

Figure 4.2: Comparison of experimental and theoretical curves, using Aluminium foils as absorption filters.

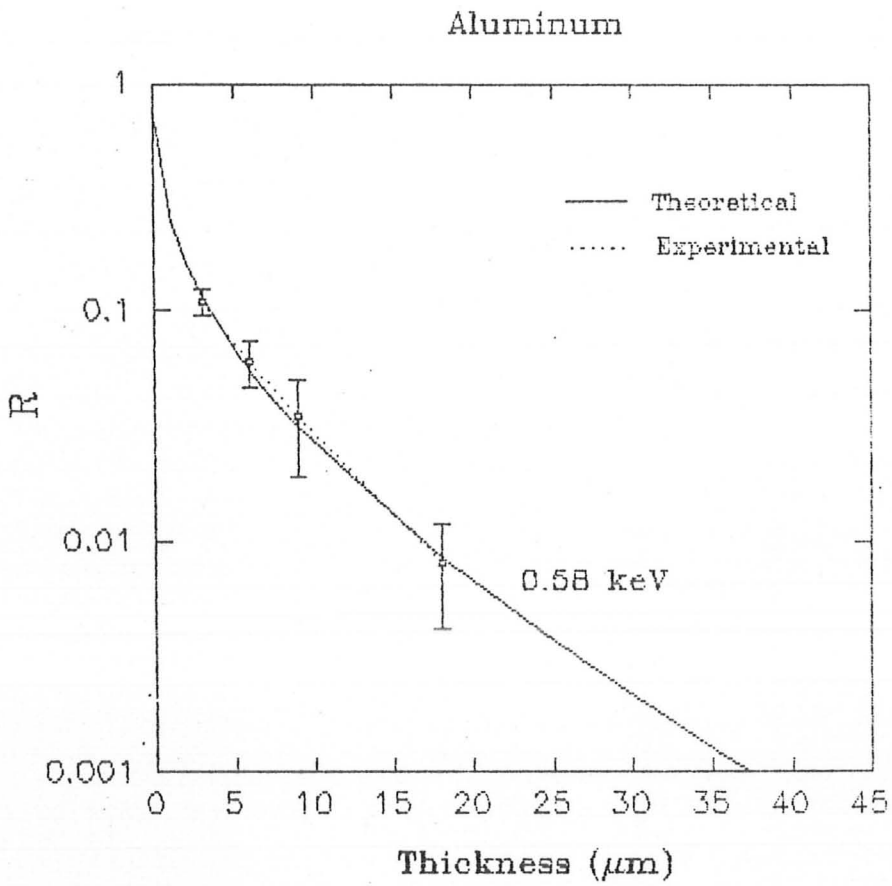

Figure 4.3: Comparison of experimental and theoretical curves, using Aluminium foils as absorption filters.

Bibliography

[1] Reviewed in; N.V.Filippov, Sov.J.Plasma Phy. **9** (1983)14.

[2] J.W.Mather, Phys. Fluids suppl. **7** (1964) S28.

[3] M.Zakaullah, T.J.Beg, S.Beg, and G.Murtaza, Phys.Lett. **A137** (1989) 39.

[4] Farhat N.Beg, M.Zakaullah, M.M.Beg and G.Murtaza. Physica Scripta. **46** (1992) 152.

[5] Farhat N. Beg, M.Zakaullah, M.Nisar and G.Murtaza. Mod. Phys. Lett. **B6** (1992) 593.

[6] M.Nisar, F.Y.Khattak, G.Murtaza, M.Zakaullah and N.Rashid. Physica Scripta. **47** (1993) 814.

[7] M.Zakaullah, Imtiaz Ahmad, Nasir Rashid, G.Murtaza and M.M.Beg. Plasma Phys., Control Fusion **35** (1993) 689.

[8] M.Zakaullah, Imtiaz Ahmad, G.Murtaza, M.Yasin, and M.M.Beg. Fusion Engg. and Design **23** (1993) 359.

[9] F.C.Jahoda, E.M.Little, W.E.Quinn, G.A.Sawyer, and T.F.Stratton, Phys.Rev. **119** (1960) 843.

[10] M.H.Key, J.Phys.B:Atom Molec.Phy. **8** (1975) 674.

[11] Yoshinobu Matsukawa, Jap.J.Appl. Phys. **16** (1977) 311.

[12] T.P.Donaldson, Plasma Phys. **20** (1978) 1279.

[13] N.Ahmad and M.H.Key, J.Phys.B:Atom Molec.Phys. **5** (1972) 866.

[14] H.R Griem, Plasma Spectroscopy McGraw-Hill, New York (1964) 193.

[15] A.B.Rodrigo, Procs.Spring college on Plasma Phys.ICTP Triestly Italy, **H4-SMR** 554/6 (1991).

[16] R.C.Elton,"Determination of Electron Temperature between 500 keV and 100 keV from X-ray Continuum Radiation in Plasmas" NRL Rep. **6738** (1968)1.

[17] B.L.Henke, P.Lee, T.J.Tanaka, R.L.Shima Bukuru and B.K.Fujikawa, Atomic Data and Nucl. Data Tables **27** (1982) 1.

[18] M.zakaullah, Samia Kausar, Imtiaz Ahmad and G.Murtaza. Mod. Phys. Lett. **B7** (1993) 835.

[19] J.W.Mather, Phys. Fluids. 8 (1965) 366.